A Theoretical Study of Excited State Properties of Adenine−Thymine and Guanine−Cytosine Base Pairs

M. K. Shukla and Jerzy Leszczynski*

Computational Center for Molecular Structure and Interactions, Department of Chemistry, Jackson State University, 1400 J. R. Lynch Street, Jackson, Mississippi 39217

Received: December 13, 2001; In Final Form: February 25, 2002

Geometries of the Watson−Crick adenine−thymine (AT) and guanine−cytosine (GC) base pairs were optimized in the ground and some selected low-lying singlet $\pi-\pi^*$ and $n-\pi^*$ excited states. Ground-state geometries were optimized at the Hartree−Fock level of theory without symmetry restriction. Excited states were generated by employing a configuration interaction technique involving singly excited configurations (CIS method) using the ground-state optimized geometry, and this was followed by excited-state geometry optimization under planar symmetry. The standard 6-31++G(d,p) basis set was employed in all calculations. Ground-state geometries are found to be planar; the predicted planarity was validated by the harmonic vibrational frequency calculations. Electronic excitations are found to be localized at either of the monomeric units. The existence of higher energy charge-transfer type excited states is also revealed. These states are characterized by the excitation of electrons from occupied orbitals of one moiety to virtual orbitals of the complementary moiety of the base pair. Electronic excitations and subsequent geometrical relaxations of base pairs in which excitations are localized at the pyrimidine moieties (thymine or cytosine) reveal a large increase in the C5C6 bond length of the pyrimidine bases. Furthermore, $n-\pi^*$ excitations are found to destabilize hydrogen bonding structures.

1. Introduction

Sequence-specific base pairing in DNA is encoded by specific hydrogen bonding patterns of adenine−thymine (AT) and guanine−cytosine (GC) base pairs. In both pairs the bases are in their normal keto-amino tautomeric forms. However, mispairing of the hydrogen bonding patterns can take place due to the formation of a minor tautomeric form through proton transfer, which may eventually lead to spontaneous mutation.[1] The formation of rare tautomeric forms can occur in the ground state or in different excited states. The latter process is even more significant since we are continuously exposed to different types of irradiation. High level theoretical investigations on some popular proton-transfer model species have predicted barrierless proton transfer in the lowest singlet $\pi-\pi^*$ excited state.[2] It is well-known that ultraviolet radiation photostimulates DNA with the formation of pyrimidine dimers. Such dimers formed between two adjacent thymine bases in the same DNA strand are the most common damage.[3]

Studies of natural DNA bases have always been very fascinating for various scientific communities to unravel the evolution of life. Different experimental and theoretical investigations have been performed on nucleic acid bases, base pairs, their model compounds, and their interactions with different solvents.[4−9] It is now well-known that these molecules are present in different tautomeric forms, and their proportion depends on the nature of the solvents. For adenine the N9H and N7H forms are the only tautomers accessible at room temperature.[9] The guanine (purine base) exhibits both the keto−enol and prototropic tautomerizms.[8,9a,10,11] The ratio of the keto−enol forms has been found to be sensitive to the molecular environment.[10] The two forms of guanine may occur in nearly equal abundance in an inert argon matrix, but the keto form is dominantly present in polar media.[8b,c,10] High level ab initio calculations on guanine and cytosine, in which the geometries were optimized at the MP2 level and higher order correlation corrections to energy were performed up to the MP4(SDTQ) or CCSD(T) level predicted numerous tautomers with close energies.[8,9a,11] At the MP2/6-31G(d) level, the keto-N7H form of guanine is slightly more stable than the keto-N9H form, and it is followed by the stability of the enol-N9H form.[8a,b,9a] Under aqueous solvation the tautomeric equilibrium is shifted toward the keto-N9H form.[8b,c,9a,11a] Consequently, the keto-N9H tautomer is found to be most stable. These calculations are in good correspondence with the experimental results on the distribution of isolated tautomers in argon and nitrogen matrixes.[10] Among pyrimidine bases, uracil and thymine are generally believed to have only the keto tautomer thermally accessible at the room temperature while cytosine exists in different tautomeric forms under various environments.[4a,5d,11,12] Although in a recent experimental study of thymine in aqueous environment at the room temperature the existence of a trace amount of the enol tautomer is also suggested.[5g] Such tautomer is excited by 295−300 nm radiation, the fluorescence of which is observed at 405 nm.[5g] While in the gas phase and in a solid matrix the enol form of cytosine is the most stable, in a polar solvent the keto form is prominent.[4a,5d,11,12]

Photophysical properties of nucleic acids are very complex and influenced by varieties of factors such as tautomerization, substitutions, surrounding environments, and stacking interactions. Spectroscopic methods including UV/vis absorption and emission as well as linear and circular dichroism are known to be important tools for monitoring nucleic acid structures and

10.1021/jp014516w CCC: $22.00
Published on Web 04/17/2002

dynamics. To explain absorption spectra, vertical transitions at the ground-state minima are needed; however, the knowledge of the relaxed singlet excited state is necessary to explain fluorescence spectra. Analyses of absorption and emission spectra are complicated by the existence of more than one tautomeric form, by a change in the solvent environment, or by substitutions of many DNA bases.[13] For example, the existence of different tautomers is necessary to explain absorption spectra of adenine and guanine while the major part of fluorescence is attributed to the N7H tautomer of respective bases.[4a,13a,14] The existence of close lying states causes geometrical deformations that enhance radiationless processes,[15] the preferential intersystem crossing,[16] or that emission occurs from only one of the two close lying singlet π- π^* or n$-\pi^*$ states.[17] The excitation of alternating polynucleotide poly(dA-dT).poly(dA-dT), a model system for double-stranded nucleic acids at the 293 nm, gives two fluorescence peaks near 330 and 410 nm.[18] However, the room temperature fluorescence spectrum of the nonalternating ploynucleotide polydA.polydT has only one fluorescence peak at about 325 nm.[19] The short wavelength emission is the result of the emission from a thymine moiety, while the long wavelength emission originates from an excited-state complex (excimer).[18,19] The formation of the excited-state complex (excimer) is the same regardless of the excitation of adenine or thymine.[18,19] It has been argued that an excited adenine forms a fluorescent excited-state complex (excimer) with an adjacent ground-state thymine in the alternating polynucleotide while in nonalternating polynucleotide (poly-dA.polydT) an excited adenine (or thymine) adjacent to another adenine (or thymine) forms a nonfluorescent complex (excimer).[18,19] Further, photophysical investigations of the synthetic polynucleotides suggest that thymine is the major emitting fluorophore in DNA[20] and is exposed to a variety of environments during the lifetime of their excited states. The fluorescence quantum yield of thymidine is found to decrease with an increase in the polarizability of the solvent, whereas it decreases with an increase in the solvent polarity and viscosity.[20] In DNA, base stacking of thymine has two opposite effects: the dispersion interactions cause fluorescence reduction and on the other hand reduction of motion of base due to stacking results in the fluorescence enhancement.[20] Geometry optimization calculations using AM1 Hamiltonian on the lowest excited dimer (excimer) singlet state of cytosine predicted a binding energy of 3 kcal/mol.[21] The excimer fluorescence was predicted to be 150 nm red-shifted relative to the monomer fluorescence. The excimer geometry was found to be distorted planes nonparallel with the C5C6 bonds in close contact. It is interesting to note that the excimer was predicted to be unstable for the planar structure and in the triplet state.[21] Chandra and Lim[22] have also found that triplet excimer states of aromatic systems are unbound or only weakly bound.

In our earlier work on the adenine-uracil (AU) base pair we have shown that electronic transitions are localized at either of the monomeric units.[23] The $\pi-\pi^*$ transitions of individual monomers are found to be unaffected under base pair formation; however, n$-\pi^*$ transitions are blue-shifted consequence to base pair formation. At least one charge-transfer type singlet excited state was found in the AU base pair. In the present work, we have carried out a geometry optimization study of adenine−thymine (AT) and guanine−cytosine (GC) base pairs in the ground and different singlet excited states. It is well-known that the real systems of nucleic acids are much more complex. In such systems base stacking and surrounding environments play a dominant role. A study of such complex systems together is still beyond the present level of computational resources. It is a reasonable approach to start from individual bases and move to base pair complexes. Here, we intend to examine the effects on spectral transitions of individual bases under base pair formation and on the stability of these complexes in different excited minima. The present study of AT and GC base pairs sheds light on the photophysical behavior of nucleic acids and is a step forward toward a better understanding of nucleic acid structures and properties both in the ground and excited states.

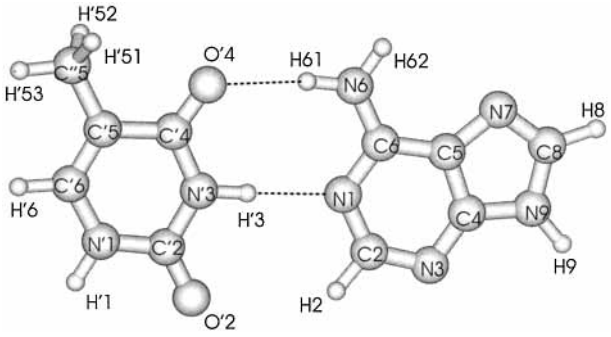

Figure 1. Atomic numbering schemes in the AT base pair.

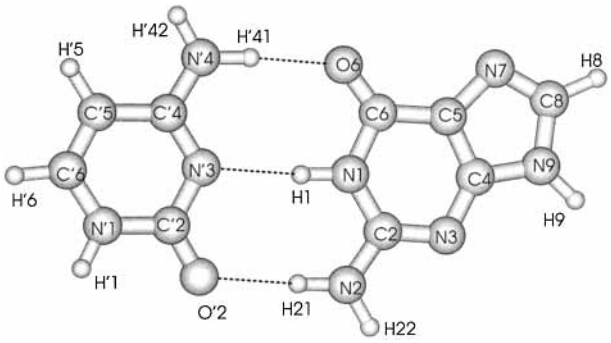

Figure 2. Atomic numbering schemes in the GC base pair.

2. Computational Details

Ground-state geometries of the Watson−Crick AT and GC base pairs (Figures 1 and 2, respectively) were optimized using the ab initio restricted Hartree−Fock method. The excited states were generated using the configuration interaction considering single electron excitations (CIS) from filled to unfilled molecular orbitals using the optimized ground-state geometry, and this was followed by geometry optimizations in the different excited states. The standard 6-31++G(d,p) basis set was used in all calculations. The nature of the ground-state potential energy surface was analyzed by vibrational frequency calculations. Due to the large size of the considered species, the excited-state geometries were optimized under the C_s symmetry. In the CIS calculation[24] all occupied and unoccupied molecular orbitals were considered using the option CIS=FULL.

The CIS method is considered as the zeroth-order approximation to study the excited-state potential energy surface and is the HF analogue for excited-state calculations.[24] It has been successfully applied to studies of excited-state properties including geometries of variety of molecules;[7,23,25,26] however, a scaling factor is needed in order to compare the results with experimental data.[7,23,25] Recently, the Tomasi group has performed computational investigations on adenine, 2-aminopurine,[27a] and guanine[27b] in which they have applied the CIS method to optimize the excited-state geometries in the gas phase and in aqueous solution while vertical transition energies were com-

TABLE 1: Vertical Excitation Energies (ΔE_{AT}, ΔE_A, ΔE_T, $\Delta E_{A(at)}$, $\Delta E_{T(at)}$, in eV), Oscillator Strength (f), and Assignments of Adenine (A), Thymine (T), and AT Base Pairs

AT[a]	A[b]		T[b]	
state/assignment/ΔE_{AT} (f)	$\Delta E_{A(AT)}$ (f)	ΔE_A (f)	$\Delta E_{T(AT)}$ (f)	ΔE_T (f)
$S_1(\pi-\sigma^*)$ 6.16(0.0057) (A*)	6.19 (0.0074)	6.19 (0.0076)		
$S_2(\pi-\pi^*)$ 6.39(0.5179) (A*)	6.43 (0.4126)	6.42 (0.4186)		
$S_3(\pi-\pi^*)$ 6.49(0.1825) (T*)[c]			6.49 (0.4409)	6.51 (0.4400)
$S_4(\pi-\sigma^*)$ 6.49(0.0037) (T*)			6.51 (0.0041)	6.54 (0.0041)
$S_5(\pi-\pi^*)$ 6.52(0.1842) (A*)	6.56 (0.0214)	6.56 (0.0236)		
$S_6(n-\pi^*)$ 6.67(0.0001) (T*)			6.43 (0.0)	6.47 (0.0)
$S_7(\pi-\sigma^*)$ 6.69(0.0000) (A*)	6.59 (0.0003)	6.60 (0.0004)		
$S_8(\pi-\sigma^*)$ 6.96(0.0043) (A*)	6.97 (0.0033)	6.97 (0.0032)		
$S_9(\pi-\pi^*)$ 7.22(0.0218) (A → T*)[d]	7.28 (0.0178)	7.28 (0.0157)		
$S_{10}(n-\pi^*)$ 7.28(0.0006) (A*)	7.13 (0.0005)	7.14 (0.0005)		
$S_{11}(\pi-\sigma^*)$ 7.33(0.0042) (T*)			7.38 (0.0045)	7.40 (0.0046)
$S_{12}(\pi-\sigma^*)$ 7.35(0.0000) (A*)	7.20 (0.0006)	7.21 (0.0007)		
$S_{13}(\pi-\sigma^*)$ 7.59(0.007) (T*)			7.60 (0.0002)	7.63 (0.0003)

[a] A* and T* indicate that the corresponding moiety of the base pair is excited. A → T* indicates excitation from adenine to thymine moiety. [b] $\Delta E_{A(AT)}$ represents the excitation energies of adenine within the geometrical framework of the optimized AT base pair geometry, while ΔE_A represents the excitation energies of separately optimized adenine moiety. Similar definition holds for $\Delta E_{T(AT)}$ and ΔE_T also. [c] Slightly contaminated by excitation of adenine unit also. [d] Slightly contaminated by the excitation to virtual orbitals of the adenine moiety.

TABLE 2: Vertical Excitation Energies (ΔE_{GC}, ΔE_G, ΔE_C, $\Delta E_{G(GC)}$, $\Delta E_{C(GC)}$, in eV), Oscillator Strength (f), and Assignments of Guanine (G), Cytosine (C), and GC Base Pair

GC[a]	G[b]		C[b]	
state/assignment/ΔE_{GC} (f)	$\Delta E_{G(GC)}$ (f)	ΔE_G (f)	$\Delta E_{C(GC)}$ (f)	ΔE_C (f)
$S_1(\pi-\sigma^*)$ 5.66(0.0005) (G*)	5.70 (0.0004)	5.85 (0.0009)		
$S_2(\pi-\sigma^*)$ 6.21(0.0101) (G*)	6.08 (0.0071)			
$S_3(\pi-\pi^*)$ 6.27(0.1449) (G*)	6.23 (0.2908)	6.21 (0.1113)		
		6.29 (0.1850)		
$S_4(\pi-\pi^*)$ 6.42(0.3199) (C*)			6.19 (0.1508)	6.21 (0.1701)
$S_5(\pi-\sigma^*)$ 6.49(0.0006) (G*)	6.59 (0.0004)	6.76 (0.0772)		
$S_6(\pi-\pi^*)$ 6.53(0.3072) (G*)	6.62 (0.3166)	6.71 (0.2375)		
$S_7(\pi-\sigma^*)$ 6.61(0.0130) (C*)			6.37 (0.0143)	6.35 (0.0139)
$S_8(\pi-\sigma^*)$ 6.80(0.0043) (G → C*)[c]	6.67 (0.0032)	6.86 (0.0024)		
$S_9(\pi-\sigma^*)$ 6.83(0.0004) (G → C*)[c]				
$S_{10}(\pi-\pi^*)$ 7.08(0.2664) (G → C*)[c]	7.14 (0.2327)	7.26 (0.1785)		
$S_{11}(\pi-\sigma^*)$ 7.10(0.0007) (G → C*)[c]	7.00 (0.0005)	7.15 (0.0118)	7.05 (0.0015)	7.04 (0.0013)
$S_{12}(n-\pi^*)$ 7.29(0.0010) (G*)	6.86 (0.0003)	6.92 (0.0010)		
$S_{13}(\pi-\sigma^*)$ 7.33(0.0020) (C*)				

[a] G* and C* indicate that the corresponding moiety of the base pair is excited. G → C* indicates that excitation from guanine to cytosine moiety. [b] $\Delta E_{G(GC)}$ represents the excitation energies of guanine within the geometrical framework of the optimized GC base pair geometry, while ΔE_G represents the excitation energies of separately optimized guanine moiety. Similar definition holds for $\Delta E_{C(GC)}$ and ΔE_C also. [c] Slightly contaminated by the excitation to virtual orbitals of guanine moiety.

puted using the time-dependent density functional theory (TDDFT) and the multireference perturbation configuration interaction (CSIPI) method utilizing the ground (at the B3LYP level) and excited-state optimized geometries employing the cc-pVDZ basis set. They have found that computed transition energies (absorption and emission) are in excellent agreement with experimental data.[27]

Ground- and excited-state basis set superposition error (BSSE) corrected interaction energies were computed using the Boys−Bernardi counterpoise correction schemes.[28] The interaction energy (E_{int}) in the ground state was calculated using the formula

$$E_{int} = E(XY) - E(X_{XY}) - E(Y_{XY}) \qquad \text{(i)}$$

where $E(XY)$ is the total energy of the XY base pair in the ground state and $E(X_{XY})$ and $E(Y_{XY})$ are the total energies of X (adenine in case of the AT base and guanine in the case of the GC base pair) and Y (thymine in the case of the AT base pair and cytosine in the case of the GC base pair) monomeric moieties, respectively, within the framework of the optimized XY base pair geometry while ghost atoms were added in place of the complementary base of the complex. The interaction energy in the excited state ($E^{(n)}_{int}$) where the excitation is localized at the X monomeric moiety was calculated using the formula

$$E^{(n)}_{int} = E^{(n)}(XY) - E^{(n')}(X_{XY}) - E^{(0)}(Y_{XY}) \qquad \text{(ii)}$$

while for the excited state where the excitation is localized at the Y monomeric moiety, the interaction energy was calculated using the formula

$$E^{(n)}_{int} = E^{(n)}(XY) - E^{(0)}(X_{XY}) - E^{(n')}(Y_{XY}) \qquad \text{(iii)}$$

In these equations ((ii) and (iii)), $E^{(n)}(XY)$ is the total energy of the XY base pair in the nth excited state and $E^{(n')}(X_{XY})$ and $E^{(n')}(Y_{XY})$ are the total energies of X and Y monomeric moieties, respectively, in the n'th excited state that corresponds to the nth state of the XY base pair (since the nth state of the XY base pair may not necessarily corresponds to the nth state of X or Y monomer; see Tables 1 and 2 and the discussion of vertical excitations). $E^{(0)}(X_{XY})$ and $E^{(0)}(Y_{XY})$ are the ground-state total energies of the X and Y monomeric moieties, respectively. In these calculations the geometries of the X and Y monomeric moieties are those within the framework of the optimized geometry of the XY base pair in the nth excited state while

ghost atoms were added in place of the complementary base of the complex. All calculations were performed using the Gaussian 94 program.[29]

3. Results and Discussion

The ground-state optimized geometries of the AT and GC base pairs are found to be planar at the HF/6-31++G(d,p) level. The predicted planarity was validated by the harmonic vibrational frequency analysis; all vibrational modes were found real. To evaluate the geometrical deformation consequent to the base pair formation, the geometries of individual bases under the constraint of planarity were also optimized at the same level of theory (HF/6-31++G(d,p)). The deformation energy calculated as the energy difference between the separately optimized isolated base (planar symmetry) to that within the framework of the optimized base pair unit shows that the geometrical deformation is small in going from individual bases to the base pair complexes. It is the lowest for adenine and the highest for cytosine. The deformation energy computed for adenine, thymine, guanine, and cytosine was found to be about 0.20, 0.33, 0.85, and 1.01 kcal/mol, respectively.

3.1. Vertical Excitations. The thirteen lowest vertical singlet excitation energies, oscillator strength, and their assignments of the AT and GC base pairs are presented in Tables 1 and 2, respectively. The transitions are characterized by either of the $\pi-\sigma^*$, $\pi-\pi^*$, or $n-\pi^*$ type and are generally localized at either of the bases. However, some transitions are of the mixed type and characterized by the excitation of electron from the occupied orbitals of one base to the virtual orbitals of the complimentary base. In an experimental study of the AT, GC polymers, and natural DNA, electronic transitions were also assigned to the corresponding monomer bases.[30] Comparison of the ground and different excited-state electronic spatial extent $\langle R^2 \rangle$ values suggested that all the $\pi-\sigma^*$ states have Rydberg character. Surprisingly the lowest singlet excited state of the AT and GC base pairs has $\pi-\sigma^*$ character and they are localized at the respective purine moiety of the base pairs (Tables 1 and 2). The possible reason that they have not been observed earlier in the transition energy calculations of isolated bases may be due the fact that basis set without diffuse function was used in calculations[6c] or in the case of CASSCF calculations the σ^* orbitals were not present in the active space.[14b] The lowest singlet excited-state $S_1(\pi-\sigma^*)$ of the AT and GC base pairs are dominated by the configuration $H \rightarrow L + 1$ and $H \rightarrow L + 2$, respectively, where H represents HOMO and L represents LUMO. The $L + 1$ and $L + 2$ orbitals are of the σ symmetry and localized along the N9H and C8H bonds of purine moieties. Such orbitals have earlier been characterized as σ^* Rydberg-type, and the corresponding $\pi-\sigma^*$ state has been characterized as not being the regular Rydberg type due to the higher polarity of such state.[31] We have also found that dipole moments of $\pi-\sigma^*$ states in the AT and GC base pairs are appreciably larger than the dipole moments of other states. The existence of a $\pi-\sigma^*$ state as a third singlet excited state in the case of indole has also been predicted at the CASSCF/CASPT2 level, and such a state lies only about 0.75 eV above the lowest singlet $\pi-\pi^*$ excited state.[31a]

To predict the extent to which base pairing affects excitations of individual bases, vertical excitation energies of individual constituents (adenine, thymine, guanine, and cytosine) within the geometrical framework of the respective optimized base pair and those corresponding to the separately optimized ground-state geometries were also computed and are presented in Tables 1 and 2. Surprisingly, at the HF/6-31++G(d,p) level the amino group of adenine and cytosine was found planar. Here, we will restrict our discussion to the $\pi-\pi^*$ and $n-\pi^*$ important types of transitions as these types of transitions of nucleic acid bases are discussed in different experimental and theoretical publications.[4−7]

In earlier studies of electronic transitions of nucleic acid bases, the computed and scaled electronic transitions obtained at the CIS level are found to be in good agreement with the corresponding experimental data.[6c,25] Broo and Holmen[6c] have computed vertical transition energies of nucleic acid bases (adenine, guanine, cytosine, uracil, thymine and some of their analogues) at the CIS/6-31G(d) and INDO/S-CI levels and compared the computed results with the available experimental data and CASSCF/CASPT2 transition energies.[6d,e,14b] They have found that the computed transition energies are differ by 0.3 eV (or less) from the corresponding experimental data.[6c] Recently, we have performed excited-state geometry optimization study of the AU base pair at the CIS/6-31++G(d,p) level.[23] We have found that the computed transition energies (after linear scaling) and transition dipole moments of adenine and uracil bases are in good agreement with the corresponding experimental data and other theoretical results obtained with more sophisticated CASPT2 calculations.[6d,14b] Therefore, here we will not discuss the electronic transitions of isolated nucleic acid bases. However, detailed study of interactions of water molecules with nucleic acid bases in the ground and $\pi-\pi^*$ and $n-\pi^*$ excited states are in progress and will be published elsewhere.

The lowest singlet $\pi-\pi^*$ excitation (S_2) of the AT base pair is characterized by an intense transition localized at the adenine moiety and is followed by a comparatively weaker $\pi-\pi^*$ transition (S_3) localized at the C′5C′6 bond of the thymine moiety of the AT base pair (Table 1). Next the $\pi-\pi^*$ transition (S_5) is also due to the excitation of the adenine moiety, the intensity being relatively weaker than the S_2 transition and similar to the S_3 transition (Table 1). The lowest singlet $n-\pi^*$ transition is the sixth transition (S_6) of the AT base pair. It is localized at the thymine moiety and originates due to the excitation of the C′4O′4 lone pair (Figure 1). In an earlier study of uracil the $n-\pi^*$ transition involving excitations out of the O4 carbonyl oxygen lone pair was predicted to be lower in energy than the transition involving excitations of the O2 carbonyl oxygen lone pair.[32] The next singlet $n-\pi^*$ excitation of the AT base pair is the tenth transition ($S_{10}(n-\pi^*)$) localized at the adenine moiety and characterized by the excitation of the nitrogen lone pair of the purine ring. The $S_9(\pi-\pi^*)$ transition of the AT base pair is similar to that of the AU base pair.[23] It is mainly characterized by the excitation from the π-type occupied orbitals of the adenine moiety to the π-type virtual orbitals localized at the thymine moiety. However, this transition is slightly contaminated by the excitation to the virtual orbitals of adenine moiety. Therefore, this excitation can be characterized as a charge-transfer type transition, giving rise to a charge-transfer type excited state (S_9). An analysis of the total Mulliken charges at the adenine moiety of the AT base pair in the ground and different $\pi-\pi^*$ and $n-\pi^*$ excited states reveals that although there is not a significant charge transfer in going from the ground state to the $S_9(\pi-\pi^*)$ excited state but it indicates the charge-transfer type nature of the state. For other states ($\pi-\pi^*$ and $n-\pi^*$) charges are approximately the same as in the ground state. The little charge-transfer contribution from the ring system to the amino group was also revealed in the twisting of the amino group of the N7H tautomer of adenine in the lowest singlet $n-\pi^*$ excited state.[25b] In this state, the

plane containing the amino group is approximately perpendicular to the plane of the ring,[25] which resembles the twisted intramolecular charge-transfer state (TICT).[5d−e,25]

A comparison of the excitation energies of the AT base pair to those of isolated monomers computed within the framework of the optimized base pair geometry shows that there is a one-to-one correspondence between the $\pi-\pi^*$ transition energies of the AT base pair and the corresponding transitions of the isolated bases (Table 1). The transition energies of the $n-\pi^*$ excitations of the AT base pair are larger than the corresponding transitions of the isolated bases (Table 1). Further, transition energies of separately optimized bases to the corresponding energies of the bases in the geometrical framework of the AT base pair are similar (Table 1). This suggests that $n-\pi^*$ transitions are blue-shifted consequent to base pair (hydrogen bonding) formation. The predicted blue shift is in accordance with the well-established fact that the $n-\pi^*$ transitions are blue-shifted under hydrogen bonding environments.[4a,b,33] The oscillator strengths of the $\pi-\pi^*$ transitions of the AT base pair where excitations are localized at the adenine moiety are increased compared to the respective transitions of the adenine moiety (Table 1). On the contrary, the oscillator strength of the $\pi-\pi^*$ transition of the AT base pair where the excitation is localized at the thymine moiety is decreased compared to the corresponding transition of the isolated thymine (Table 1). The computed first transition of thymine is found to be of the $n-\pi^*$ type, and the second is of the $\pi-\pi^*$-type (Table 1).[7c] This sequence is reversed after the base pair formation (Table 1). Subsequently, the first $n-\pi^*$ transition of the AT base pair where the excitation is localized at the thymine moiety has higher energy than the first $\pi-\pi^*$-type of transition with the excitation localized at the thymine moiety (Table 1). These findings are in accordance with the experimental observations that under the hydrogen bonding environment the nature of the lowest singlet excited state of thymine is changed from the $n-\pi^*$- to $\pi-\pi^*$-type.[4a,34]

The data presented in Table 2 show that the lowest singlet $\pi-\pi^*$ excitation of the GC base pair is the third transition (S_3) localized at the guanine moiety and is followed by a relatively more intense $\pi-\pi^*$ transition localized at the cytosine moiety. The sixth transition is also a $\pi-\pi^*$-type localized at the guanine moiety. The tenth transition is characterized by the excitation from the π-type occupied orbitals of the guanine moiety to the π^*-type virtual orbitals of the cytosine moiety. Furthermore, this transition is slightly contaminated by the excitation to the unoccupied π-type orbitals of the guanine moiety (Table 2). As discussed earlier in the case of the AT base pair, this state can also serve as a charge-transfer state. We have found only one $n-\pi^*$ transition (S_{12}) among the calculated 13 lowest singlet vertical excitations of the GC base pair studied here. This transition ($S_{12}(n-\pi^*)$) is localized at the guanine moiety and is characterized due to the excitation of the carbonyl lone pair. The higher lying $n-\pi^*$ excited states in the GC base pair is not unexpected in view of the presence of hydrogen bonds in the base pair since $n-\pi^*$ transition energies do generally increase under hydrogen bonding environments.[4a,b,33]

The $\pi-\pi^*$ excitation energies of the guanine moiety computed within the framework of the optimized geometry of the GC base pair are not significantly effected as a consequence of the base pair formation, the maximum difference being within the range of 0.1 eV. However, the $n-\pi^*$ transition energy of the guanine moiety is appreciably increased upon base pair formation. Such a rise in the $n-\pi^*$ transitions under hydrogen bonding is well-known, as discussed earlier.[4a,b,33] Unexpectedly, the transition energy of the lowest singlet $\pi-\pi^*$excitation of cytosine computed within the framework of the GC base pair is appreciably increased under the GC base pair formation (Table 2). However, the second singlet $\pi-\pi^*$ transition of cytosine is not much affected (Table 2). Such a rise in the excitation energy of the first $\pi-\pi^*$ transition may be due the influence of hydrogen bonds in the base pair. The disagreement between the transition energies of isolated guanine and cytosine bases to those of the GC base pair are more than those between the transition energies of isolated adenine and thymine to those of the AT base pair. Such differences may be due to the presence of three hydrogen bonds in the GC base pair and comparatively larger deformation in the geometry of the isolated G and C bases as discussed earlier. Table 2 also suggests that transition energies calculated for the separately optimized bases (guanine and cytosine) and those with in the geometrical framework of the GC base pair are almost similar. In the case of transition energy calculations of guanine (optimized separately in the ground state) some Rydberg contamination was also found. Such contamination may be due to the nonplanarity of system in the ground state.

3.2. Excited-State Geometries. The geometry of the AT base pair was optimized for the lowest two singlet $\pi-\pi^*$ (S_2 and S_3) and lowest two singlet $n-\pi^*$ (S_6 and S_{10}) excited states using the CIS method.[24] They are the lowest singlet excited state of either of the $\pi-\pi^*$ or $n-\pi^*$ type localized at the adenine or thymine moieties under the AT base pair excitations. The optimized bond lengths and bond angles (for heavy atoms) in these excited states along with the optimized ground-state parameters are presented in Table 3. As the $S_2(\pi-\pi^*)$ excitation is localized at the adenine moiety, the geometrical changes consequent to state relaxation are revealed in the adenine moiety in going from the ground state to the $S_2(\pi-\pi^*)$ excited state while no significant changes are observed in the geometry of the thymine moiety (Table 3). The prominent changes are localized at the C2═N3─C4═C5─N7═C8 and C5─C6 fragments of adenine. As compared to the respective ground-state values, the C2N3, C4C5, C5C6, and N7C8 bond lengths are increased in the range of 0.05−0.08 Å while the N3C4 and C5N7 bond lengths are decreased by about 0.048 and 0.066 Å, respectively (Table 3). Thus, the characters of single and double bonds in the C2═N3─C4═C5─N7═C8 fragment are interchanged. Interestingly, the C5C6 bond length is further increased by about 0.052 Å in this state. The geometrical distortion is similar to those found in the lowest singlet $\pi-\pi^*$ excited state of the N9H tautomer of adenine.[25a] A similar change was also revealed in the geometry of the AU base pair in the lowest singlet $\pi-\pi^*$ excited state, the excitation being localized at the adenine moiety.[23]

As discussed earlier, the $S_3(\pi-\pi^*)$ excitation of the AT base pair is localized at the thymine moiety; consequently, geometrical change is revealed at this moiety under state relaxation. As compared to the ground state the alternate "increase and decrease" in the ring bond lengths of thymine is predicted; the most significant change being the large increase of the C′5C′6 bond length by about 0.125 Å (Table 3). The large increase of this bond length is in accordance with the excitation being localized mainly at this bond (C′5C′6), as discussed earlier. It is well-known that thymine under UV irradiation forms a photodimer through the C5C6 bond.[4a,b] Thus the increase in the C′5C′6 bond length is also in accordance with the reactivity of the molecule under electronic excitation. In an earlier theoretical study of excited states of different pyrimidines, the geometrical distortions in the lowest singlet $\pi-\pi^*$ excited state of thymine and cytosine were found to be very large, especially

TABLE 3: Ground and Excited State Optimized Bond Lengths (Å) and Bond Angles (deg) of the AT Base Pair

bond length	S_0	$S_2(\pi-\pi^*)$	$S_3(\pi-\pi^*)$	$S_6(n-\pi^*)$	$S_{10}(n-\pi^*)$
N1−C2	1.333	1.322	1.332	1.337	1.378
C2−N3	1.311	1.389	1.311	1.311	1.371
N3−C4	1.332	1.284	1.332	1.329	1.315
C4−C5	1.375	1.428	1.375	1.376	1.380
C5−C6	1.404	1.456	1.405	1.401	1.445
N1−C6	1.334	1.322	1.336	1.329	1.290
C5−N7	1.382	1.316	1.382	1.382	1.367
N7−C8	1.282	1.343	1.282	1.282	1.279
C8−N9	1.371	1.370	1.371	1.371	1.388
C4−N9	1.361	1.378	1.361	1.361	1.353
C6−N6	1.333	1.330	1.332	1.340	1.345
N′1−C′2	1.369	1.370	1.397	1.363	1.369
C′2−N′3	1.367	1.369	1.354	1.361	1.369
N′3−C′4	1.376	1.375	1.402	1.414	1.377
C′4−C′5	1.469	1.468	1.424	1.449	1.469
C′5−C′6	1.332	1.333	1.457	1.335	1.332
N′1−C′6	1.375	1.374	1.343	1.402	1.375
C′2−O′2	1.199	1.197	1.197	1.205	1.197
C′4−O′4	1.206	1.207	1.225	1.274	1.204
C′5−C”5	1.503	1.503	1.483	1.504	1.503
bond angles	**S_0**	**$S_2(\pi-\pi^*)$**	**$S_3(\pi-\pi^*)$**	**$S_6(n-\pi^*)$**	**$S_{10}(n-\pi^*)$**
N1C2N3	128.3	126.5	128.4	127.9	113.6
C2N3C4	111.7	113.2	111.6	112.0	122.8
N3C4C5	126.6	126.6	126.6	126.5	123.0
C4C5C6	116.5	115.1	116.6	116.3	115.3
C5C6N1	117.6	118.0	117.5	118.2	117.8
C2N1C6	119.3	120.7	119.3	119.1	127.5
C4C5N7	110.9	112.3	110.9	111.0	110.5
C5N7C8	104.3	105.3	104.3	104.2	105.6
N7C8N9	113.4	111.9	113.4	113.5	112.2
C8N9C4	106.5	107.3	106.5	106.5	106.4
C5C4N9	104.9	103.3	104.9	104.8	105.3
N6C6C5	122.7	119.8	122.8	122.1	120.2
N′1C′2N′3	114.1	113.9	115.8	115.4	113.8
C′2N′3C′4	126.7	126.7	124.8	123.2	126.9
N′3C′4C′5	116.0	116.1	117.0	119.2	115.8
C′4C′5C′6	117.2	117.1	119.7	116.4	117.2
C′5C′6N′1	122.8	122.8	116.5	121.8	122.8
C′6N′1C′2	123.2	123.3	126.2	124.1	123.3
O′2C′2N′3	123.4	123.5	125.0	122.1	123.4
O′4C′4N′3	120.5	120.5	118.9	117.1	120.5
C”5C′5C′4	118.4	118.5	120.3	119.8	118.4

TABLE 4: Ground and Excited State Optimized Bond Lengths (Å) and Bond Angles (deg) of the GC Base Pair

bond length	S_0	$S_3(\pi-\pi^*)$	$S_4(\pi-\pi^*)$
N1−C2	1.361	1.374	1.360
C2−N3	1.304	1.328	1.302
N3−C4	1.345	1.311	1.346
C4−C5	1.374	1.455	1.374
C5−C6	1.427	1.417	1.428
N1−C6	1.395	1.423	1.397
C5−N7	1.382	1.357	1.381
N7−C8	1.278	1.303	1.278
C8−N9	1.378	1.351	1.377
C4−N9	1.354	1.385	1.354
C6−O6	1.212	1.223	1.210
C2−N2	1.337	1.335	1.340
N′1−C′2	1.387	1.388	1.424
C′2−N′3	1.349	1.347	1.334
N′3−C′4	1.315	1.315	1.350
C′4−C′5	1.447	1.447	1.405
C′5−C′6	1.338	1.339	1.445
N′1−C′6	1.354	1.354	1.342
C′2−O′2	1.212	1.213	1.208
C′4−N′4	1.324	1.325	1.345
bond angles	**S_0**	**$S_3(\pi-\pi^*)$**	**$S_4(\pi-\pi^*)$**
N1C2N3	123.4	124.5	123.6
C2N3C4	112.7	115.0	112.7
N3C4C5	128.9	125.8	128.9
C4C5C6	117.9	119.0	118.0
C5C6N1	111.1	112.3	111.0
C2N1C6	125.9	123.5	125.8
C4C5N7	110.6	109.2	110.6
C5N7C8	104.8	105.6	104.8
N7C8N9	112.9	115.0	112.9
C8N9C4	106.6	106.2	106.6
C5C4N9	105.1	104.1	105.2
O6C6C5	129.5	129.6	129.6
N2C2N1	116.4	116.3	116.5
N′1C′2N′3	117.7	117.6	120.2
C′2N′3C′4	121.0	121.2	119.2
N′3C′4C′5	122.0	121.9	122.1
C′4C′5C′6	116.3	116.3	119.7
C′5C′6N′1	120.6	120.6	115.0
C′6N′1C′2	122.4	122.3	123.7
O′2C′2N′3	123.8	123.8	124.9
N′4C′4N′3	118.3	118.2	116.7

around the C5C6 bond; the length of this bond is also increased appreciably.[7c] The large increase in the C′5C′6 bond length of thymine consequent to the singlet $\pi-\pi^*$ excitation can be related to the photodimerization of pyrimidines in which the singlet excimer state has been suggested as a precursor.[21,35]

In the $S_6(n-\pi^*)$ excited state, the N′1C′6 and N′3C′4 bond lengths are increased by 0.027 and 0.038 Å, respectively, while the C′4C′5 bond length is decreased by 0.02 Å compared to the respective ground-state value (Table 3). The largest change is found in the C′4O′4 bond, which is increased by 0.068 Å. Such an increase is in accordance with the excitation being localized mainly at this carbonyl group. Similar changes are also revealed in an earlier study of the lowest singlet $n-\pi^*$ excited state of thymine; the geometry was also predicted to be highly nonplanar.[7c] However, it should be noted that the present study has been performed under C_s symmetry in the excited state.

In the $S_{10}(n-\pi^*)$ excited state, significant changes are localized mainly at the N3=C2−N1=C6−C5 fragment of the adenine base. The N1C6 bond length is decreased by about 0.044 Å, while the N1C2, C2N3, and C5C6 bond lengths are increased by about 0.045, 0.06, and 0.041 Å, respectively. An appreciable change in the bond angles is also revealed in this state: the N1C2N3 bond angle is decreased by about 14.7°, while the C2N3C4 and C2N1C6 bond angles are increased by 11.2° and 8.2°, respectively (Table 3).

The geometries of the GC base pair optimized in the $S_3(\pi-\pi^*)$ and $S_4(\pi-\pi^*)$ excited states are presented in Table 4 along with the ground-state geometry. As discussed earlier, these states correspond to the lowest singlet $\pi-\pi^*$ excited state where the excitation is localized at the guanine (S_3) and cytosine (S_4) moieties. In going from the ground state to the $S_3(\pi-\pi^*)$ excited state, a geometrical deformation was found in the guanine ring. The ring bond lengths are generally found to increase or decrease in the range of 0.024−0.034 Å, except for the N1C2 and C5C6 bonds. These bond lengths (N1C2 and C5C6) are found to increase and decrease by 0.013 and 0.01 Å, respectively. Maximum increase by 0.081 Å is revealed in the C4C5 bond length. Furthermore, the C6O6 bond length is also found to increase by 0.011 Å (Table 4). In an excited-state geometry optimization study of guanine tautomers, similar changes were observed in the lowest singlet $\pi-\pi^*$ excited state of the N9H tautomer of guanine.[25c] In the $S_4(\pi-\pi^*)$ excited state of the GC base pair where the excitation is localized at the cytosine moiety, the alternate ring bond length of cytosine is found to increase and decrease compared to the respective ground-state values (Table 4). The C′5C′6 bond length is found to increase appreciably by about 0.107 Å.

TABLE 5: Hydrogen Bond Lengths (Å) and Hydrogen Bond Angles (deg) of the AT and GC Base Pairs in the Ground and Different Excited States

	states				
parameters	S_0	$S_2(\pi-\pi^*)$	$S_3(\pi-\pi^*)$	$S_6(n-\pi^*)$	$S_{10}(n-\pi^*)$
AT Base Pair					
N6...O′4	3.083	3.011	3.027	3.778	3.094
N1...N′3	3.023	3.071	3.025	3.090	3.152
H61(N6)...O′4	2.090	2.016	2.029	2.778	2.106
N1...H′3	2.010	2.063	2.014	2.086	2.149
O′4H61N6	172.6	171.1	174.5	161.8	170.2
N′3H′3N1	177.7	174.8	177.2	183.2	174.3
E_{int}[a] (kcal/mol)	−9.9	−10.0	−10.6	−5.8	−7.1

parameters	S_0	$S_3(\pi-\pi^*)$	$S_4(\pi-\pi^*)$
GC Base Pair			
O6...N′4	2.932	2.937	2.958
N1...N′3	3.053	3.023	3.066
N2...O′2	3.028	3.037	3.098
O6...H′41(N′4)	1.926	1.929	1.954
H1(N1)...N′3	2.048	2.021	2.059
H21(N2)...O′2	2.028	2.034	2.100
O6H′41N′4	175.7	177.7	177.3
N1H1N′3	175.3	176.3	176.4
N2H21O′2	176.9	177.4	177.7
E_{int}[a] (kcal/mol)	−24.8	−22.9	−20.4

[a] Ground and excited-state interaction energies.

Several attempts were made to optimize the charge-transfer type excited states of the AT and GC the base pairs. In all attempts optimizations were found to converge to the geometry of $\pi-\pi^*$ excited state of adenine (in the AT base pair) or guanine (in the GC base pair). Attempts were also made to optimize the $S_{12}(n-\pi^*)$ excited state of the GC base pair, the excitation being localized at the guanine moiety. In all attempts, as the optimization proceeded, after a few optimization cycles, it was very difficult to trace this state, and the root of interest ($S_{12}(n-\pi^*)$) was crossed over to the different states.

3.3. Hydrogen Bonding, Interaction Energies, and Dipole Moments. The Watson−Crick AT base pair is characterized by two while the GC base pair is characterized by three hydrogen bonds. In the AT base pair, hydrogen bonds are formed between the amino group hydrogen of adenine acting as a hydrogen bond donor and the C′4O′4 group of thymine acting as hydrogen bond acceptor and between the N1 atomic site of adenine acting as a hydrogen bond acceptor and the N′3H site of thymine acting as a hydrogen bond donor (Figure 1). Similarly, in the GC base pair hydrogen bonds are formed between the carbonyl oxygen of guanine and the amino hydrogen of cytosine, the N1H site of guanine and the N′3 site of cytosine, and the amino hydrogen of guanine and the carbonyl oxygen of cytosine (Figure 2). The computed hydrogen bond distances and hydrogen bond angles of the AT and GC base pairs in the ground and different excited states are shown in Table 5. In the case of AT base pair, in going from the ground state to different excited states, the N1...H′3 hydrogen bond length is increased. Such an increase is more pronounced in the $n-\pi^*$ excited states, and especially in the $S_{10}(n-\pi^*)$ excited state where the excitation is localized at the adenine moiety (Table 5). The H61(N6)...O′4 hydrogen bond length is decreased in going from the ground state to the $\pi-\pi^*$ excited states and increased in the $n-\pi^*$ excited states. This increase is maximum (about 0.7 Å) in the $S_6(n-\pi^*)$ excited state, the excitation being localized at the thymine moiety. Such a large increase in the H61(N6)...O′4 hydrogen bond length can be attributed to the large increase in the C′4O′4 bond length in this state (S_6) and also to the fact that hydrogen bonds are destabilized in the $n-\pi^*$ excited states.[36−39] This table (Table 5) also suggests that the N1...H′3 hydrogen bond is linear within 6° in the ground and different excited states while the O4′...H61 hydrogen bond generally deviates from linearity. The deviation from linearity is maximum (about 18°) in the $S_6(n-\pi^*)$ excited state (Table 5). Again, such a large deviation from the straight line is due to the large increase in the C4′O4′ bond length in this state (Tables 3 and 5).

In the case of the GC base pair, no appreciable change in hydrogen bond lengths is revealed (Table 5) in going from the ground state to the $S_3(\pi-\pi^*)$ and $S_4(\pi-\pi^*)$ excited states. Hydrogen bonds were also found to be almost linear (within 5°) in the ground and different $\pi-\pi^*$ excited states.

Thus, the above discussion also suggests that hydrogen bonding is destabilized under $n-\pi^*$ excitations. A recent experimental study of the hydrated clusters of adenine in a supersonic molecular beam has shown a weakening of hydrogen bonding and subsequent fragmentation of adenine monomer hydrated clusters in the $n-\pi^*$ excited state of adenine.[36] Krishna and Goodman[37] have found very weak hydrogen bonds in the triplet $n-\pi^*$ state of pyrazine and pyrimidine. In the case of diazine under methanol or a water environment, in the singlet $n-\pi^*$ state, hydrogen bonding is suggested to be dissociative[38] while it has been suggested that the $n-\pi^*$ excitation destabilizes the hydrogen bonds in the hydrated adenine clusters.[39]

Interaction energies shown in the Table 5 reveal that the AT base pair is characterized by low interaction energy. Furthermore, the ground and $\pi-\pi^*$ excited-state interaction energies of the AT base pair are found to be similar in magnitude while the $n-\pi^*$ excited state interaction energies are found to be significantly reduced (in magnitude) particularly in the $S_6(n-\pi^*)$ excited state, the excitation being localized at the thymine moiety (Table 5). As a consequence, hydrogen bonds in the AT base pair are the least stable in the $S_6(n-\pi^*)$ excited state. Thus the AT base pair would have similar stability in the ground and different singlet $\pi-\pi^*$ excited states while the stability will be significantly reduced in singlet $n-\pi^*$ excited states.

The interaction energy of the GC base pair is about 2.5 times more than that of the AT base pair (Table 5). Further, the maximum revealed interaction energy for the GC base pair is in the ground state while it is slightly reduced (in magnitude) in the $\pi-\pi^*$ excited state (Table 5). These results suggest that the GC base pair would be slightly less stable in the singlet $\pi-\pi^*$ excited states.

The ground and excited-state dipole moments of the AT and GC base pairs are presented in Table 6. This table suggests that the AT complex has the lowest dipole moment in the $S_5(\pi-\pi^*)$ excited state and the highest in the $S_9(\pi-\pi^*)$ singlet excited state. Further, the dipole moment for the $S_2(\pi-\pi^*)$ excited state is increased and, for the $S_6(n-\pi^*)$ excited state, is decreased under respective geometrical relaxation. For other states no significant change of dipole moment is revealed under geometrical relaxation. The dipole moment of the GC base pair is larger than that of the AT base pair. The GC base pair in the $S_6(\pi-\pi^*)$ state has an appreciably large dipole moment and is followed by the dipole moment of the $S_{12}(n-\pi^*)$ excited state. Interestingly, while the charge-transfer $S_9(\pi-\pi^*)$ state of the AT base pair has the highest dipole moment, the charge-transfer state ($S_{10}(\pi-\pi^*)$) of the GC base pair has the lowest dipole moment among the ground and excited-state dipole moments of the corresponding base pairs (Table 6). Further, a variation among the dipole moment of the excited states of the GC base pair is more than in the AT base pair. It is also imperative to note that such a large variation in dipole moment of the GC

TABLE 6: Computed Dipole Moment (μ, Debye) of the AT and GC Base Pairs[a]

state	μ
AT Base Pair	
S_0	2.30
$S_2(\pi-\pi^*)$	2.81 (3.67)
$S_3(\pi-\pi^*)$	2.29 (2.28)
$S_5(\pi-\pi^*)$	1.79
$S_6(n-\pi^*)$	2.94 (2.43)
$S_9(\pi-\pi^*)$	4.68
$S_{10}(n-\pi^*)$	2.15 (2.25)
GC Base Pair	
S_0	6.44
$S_3(\pi-\pi^*)$	4.99 (4.5)
$S_4(\pi-\pi^*)$	6.30 (6.31)
$S_6(\pi-\pi^*)$	10.40
$S_{10}(\pi-\pi^*)$	3.99
$S_{12}(n-\pi^*)$	9.18

[a] Dipole moments of the geometrically relaxed excited states are shown in parentheses.

base pair among different states would lead to strong rearrangement of excited states under polar solvation.

4. Conclusions

Electronic transitions are generally localized at either of the monomeric units of the GC and AT complexes. The base pair formation does not have significant effect on the singlet $\pi-\pi^*$ transitions of constituent bases; however, $n-\pi^*$ transition energies are appreciably blue-shifted. Such a blue shift is in accordance with experimental findings on $n-\pi^*$ transitions under hydrogen bonding environments. The existence of selected states of charge-transfer types lying at higher energy is also revealed. Excited-state geometry relaxations of $\pi-\pi^*$ excited states of base pairs where excitations are localized at the pyrimidine moieties lead to appreciably large increases in the C5C6 bond lengths of pyrimidines (thymine or cytosine). Such a large increase is important for photophysical activity of nucleic acids. Hydrogen bonds are found to be destabilized under $n-\pi^*$ excitations. Interaction energies are also appreciably reduced (in magnitude) in $n-\pi^*$ excited states.

Acknowledgment. We are thankful to NIH-RCMI grant No. G1 2RR13459-21, NSF-CREST grant No.9805465, and ONR grant No. N00014-98-1-0592 for financial assistance. We are also thankful to the Mississippi Center for Supercomputing Research for the computational facilities.

Supporting Information Available: Optimized ground and excited states *X*, *Y*, *Z* coordinates of the AT and GC base pair. This material is available free of charge via the Internet at http://pubs.acs.org.

References and Notes

(1) (a) Nishio, H.; Ono, A.; Matsuda, A.; Ueda, T. *Nucl. Acids Res.* **1992**, *20*, 777. (b) Strazewski, P.; Tamm, C. *Angew. Chem., Int. Ed. Engl.* **1990**, *29*, 36. (c) Singer, B.; Chavez, F.; Goodman, M. F.; Essigmann, J. M.; Dosanjh, M. K. *Proc. Natl. Acad. Sci. U.S.A.* **1989**, *86*, 8271.

(2) Sobolewski, A. L.; Domcke, W. *Chem. Phys. Lett.* **1999**, *300*, 533.

(3) (a) Darnell, J.; Lodish, H.; Baltimore, D. *Molecular Cell Biology*, Scientific American Books, New York, 1986; pp 553. (b) Taylor, J.-S. *Chem. Educ.* **1990**, *67*, 835.

(4) (a) Callis, P. R. *Annu. Rev. Phys. Chem.* **1983** *34*, 329. (b) Eisinger, J.; Lamola, A. A. In *Excited state of Proteins and Nucleic Acids*; Steiner, R. F., Weinryb, I., Eds.; Plenum Press: New York, London, 1971. (c) Rahn, R. O.; Yamane, T.; Eisinger, J.; Longworth, J. W.; Shulman, R. G. *J. Chem. Phys.* **1966** *45*, 2947. (d) Holmen, A.; Norden, B.; Albinson, B. *J. Am. Chem. Soc.* **1997** *119*, 3114. (e) Michl, J. *Tetrahedron* **1984**, *40*, 3845. (f) Morgan, J. P.; Daniels, M. *Photochem. Photobiol.* **1980** *31*, 101.

(5) (a) Molteni, C.; Frank, I.; Parrinello, M. *J. Am. Chem. Soc.* **1999**, *121*, 12177. (b) Proppe, B.; Merchan, M.; Serrano-Andres, L. *J. Phys. Chem. A* **2000**, *104*, 1608. (c) Merchan, M.; Serrano-Andres, L.; Gonzalez-Luque, R.; Roos, B. O.; Rubio, M. *J. Mol. Struct. (THEOCHEM)* **1998**, *463*, 201. (d) Andreasson, J.; Holmen, A.; Albinsson, B. *J. Phys. Chem. B* **1999**, *103*, 9782. (e) Albinson, B. *J. Am. Chem. Soc.* **1997**, *119*, 6369. (f) Scheiner, S. *J. Phys. Chem. A* **2000**, *104*, 5898. (g) Morsy, M. A.; Al-Somali, A. M.; Suwaiyan, A. *J. Phys. Chem. B* **1999**, *103*, 11205.

(6) (a) Callis, P. R. *Photochem. Photobiol.* **1986**, *44*, 315. (b) Borin, A. C.; Serrano-Andres, L.; Fulscher, M. P.; Roos, B. O. *J. Phys. Chem. A* **1999**, *103*, 1838. (c) Broo, A.; Holmen, A. *J. Phys. Chem. A* **1997**, *101*, 3589. (d) Fulscher, M. P.; Roos, B. O. *J. Am. Chem. Soc.* **1995**, *117*, 2089. (e) Lorentzon, J.; Fulscher, M. P.; Roos, B. O. *J. Am. Chem. Soc.* **1995**, *117*, 9265. (f) Shukla, M. K.; Mishra, P. C. *J. Mol. Struct.* **1994**, *324*, 241. (g) Shukla, M. K.; Mishra, P. C. *J. Mol. Struct.* **1996**, *377*, 247. (h) Petke, J. D.; Maggiora, G. M.; Christoffersen, R. E. *J. Am. Chem. Soc.* **1990**, *112*, 5452.

(7) (a) Shukla, M. K.; Leszczynski, J. *Int. J. Quantum Chem.* **2000**, *77*, 240. (b) Shukla, M. K.; Mishra, P. C. *Chem. Phys.* **1998**, *230*, 187. (c) Shukla, M. K.; Mishra, P. C. *Chem. Phys.* **1999**, *240*, 319. (d) Slater, L. S.; Callis, P. R. *J. Phys. Chem.* **1995**, *99*, 8572. (e) Fang, W.-H. *J. Chem. Phys.* **1999**, *111*, 5361.

(8) (a) Leszczynski, J. *J. Phys. Chem. A* **1998**, *102*, 2357. (b) Gorb, L.; Leszczynski, J. *J. Am. Chem. Soc.* **1998**, *120*, 5024. (c) Gorb, L.; Leszczynski, J. *Int. J. Quantum Chem.* **1997**, *65*, 759. (d) Hobza, P.; Sponer, J. *Chem. Rev.* **1999**, *99*, 3247. (e) Gorb, L.; Leszczynski, J. In *Computational Molecular Biology, Theoretical and Computational Chemistry Book Series*; Leszczynski, J., Ed.; Elsevier: Amsterdam, 1999; Vol. 8, pp 167. (f) Hobza, P.; Sponer, J.; Leszczynski, J. In *Computational Molecular Biology, Theoretical and Computational Chemistry Book Series*; Leszczynski, J., Ed.; Elsevier: Amsterdam, 1999; Vol. 8, pp 85. (g) Leszczynski, J. *The Encyclopedia of Computational Chemistry*; John Wiley & Sons: New York, 1998; Vol. V, pp 2951.

(9) (a) Leszczynski, J. In *Advances in Molecular Structure and Research*; Hargittai, M., Hargittai, I., Eds.; JAI Press Inc.: Stamford, CT, 2000; Vol. 6, p 209. (b) Gu, J.; Leszczynski, J. *J. Phys. Chem. A* **1999**, *103*, 2744.

(10) (a) Sheina, G. G.; Stepanian, S. G.; Radchenko, E. D.; Blagoi, Yu. P. *J. Mol. Struct.* **1987**, *158*, 275. (b) Szczepaniak, K.; Szczesniak, M.; Person, W. B. *Chem. Phys. Lett.* **1988**, *153*, 39. (c) Szczepaniak, K.; Szczesniak, M. *J. Mol. Struct.* **1987**, *156*, 29. (d) Radchenko, E. D.; Plohotnichenko, A. M.; Sheina, G. G.; Balgoi, Yu. P. *Biophysics* **1983**, *28*, 559 (Engl. Ed.). (e) Szczepaniak, K.; Szczesniak, M.; Szajda, W.; Person, W. B.; Leszczynski, J. *Can. J. Chem.* **1991**, *69*, 1705.

(11) (a) Colominas, C.; Luque, F. J.; Orozco, M. *J. Am. Chem. Soc.* **1996**, *118*, 6811. (b) Gould, I. R.; Burton, N. A.; Hall, R. J.; Hillier, I. H. *J. Mol. Struct. (THEOCHEM)* **1995**, *331*, 147.

(12) (a) Gorb, L.; Leszczynski, J. *Int. J. Quantum. Chem.* **1998**, *70*, 855. (b) Gould, I. R.; Hillier, I. H. *Chem. Phys. Lett.* **1989**, *161*, 185. (c) Gould, I. R.; Vincent, M. A.; Hillier, I. H.; Lapinski, L.; Nowak, M. J. *Spectrochim. Acta* **1992**, *48A*, 811. (d) Szczesniak, M.; Szczepaniak, K.; Kwiatkowski, J. S.; KuBulat, K.; Person, W. B. *J. Am. Chem. Soc.* **1988**, *110*, 8319. (e) Radchenko, E. D.; Sheina, G. G.; Smorygo, N. A.; Blagoi, Yu. P. *J. Mol. Struct.* **1984**, *116*, 387. (f) Nowak, M. J.; Lapinski, L.; Fulara, J. *Spectrochim. Acta* **1989**, *45A*, 229.

(13) (a) Wilson, R. W.; Callis, P. R. *Photochem. Photobiol.* **1980**, *31*, 323. (b) Dreyfus, M.; Dodin, G.; Bensaude, O.; Dubois, J. E. *J. Am. Chem. Soc.* **1975**, *97*, 2369. (c) Chenon, M. T.; Pugmire, R. S.; Grant, D. M.; Panzica, R. P.; Townsend, L. B. *J. Am. Chem. Soc.* **1975**, *97*, 4636. (d) Wilson, R. W.; Callis, P. R. *J. Phys. Chem.* **1976**, *80*, 2280. (e) Alyoubi, A. O.; Hilal, R. H. *Biophys. Chem.* **1995**, *55*, 231. (f) Mishra, P. C. *J. Mol. Struct.* **1989**, *195*, 201. (g) Santhosh, C.; Mishra, P. C. *J. Mol. Struct.* **1989**, *198*, 327.

(14) (a) Mishra, P. C.; Jug, K. *J. Mol. Struct. (THEOCHEM)* **1994**, *305*, 139. (b) Fulscher, M. P.; Serrano-Andres, L.; Roos, B. O. *J. Am. Chem. Soc.* **1997**, *119*, 6168.

(15) Lamola, A. A.; Eisinger, J. *Biochim. Biophys. Acta* **1971**, *240*, 313.

(16) Vigny, P. *C. R. Acad. Sci. Ser.* **1971**, *D272*, 3206.

(17) Hauswirth, W.; Daniels, M. *Photochem. Photobiol.* **1971**, *13*, 157.

(18) Ge, G.; Georghiou, S. *Photochem. Photobiol.* **1991** *54*, 301.

(19) Ge, G.; Georghiou, S. *Photochem. Photobiol.* **1991** *54*, 477.

(20) Georghiou, S.; Gerke, L. S. *Photochem. Photobiol.* **1999** *69*, 646,

(21) Danilov, V. I.; Slyusarchuk, O. N.; Alderfer, J. L.; Stewart, J. J. P.; Callis, P. R. *Photochem. Photobiol.* **1994**, *59*, 125.

(22) Chandra, A. K.; Lim, E. C. *J. Chem. Phys.* **1968**, *49*, 5066.

(23) Shukla M. K.; Leszczynski, J. *J. Phys. Chem.* A **2002**, *106*, 1011.

(24) Foresman, J. B.; Head-Gordon, M.; Pople, J. A.; Frisch, M. J. *J. Phys. Chem.* **1992**, *96*, 135.

(25) (a) Mishra, S. K.; Shukla, M. K.; Mishra, P. C. *Spectrochim. Acta* **2000**, *56A*, 1355. (b) A. Broo, *J. Phys. Chem. A* **1998**, *102*, 526. (c) Shukla, M. K.; Mishra, S. K.; Kumar A.; Mishra, P. C. *J. Comput. Chem.* **2000**, *21*, 1. (d) Holmen, A.; Broo, A.; Albinsson, B.; Norden, B. *J. Am. Chem. Soc.* **1997**, *119*, 12240.

(26) (a) Organero, J. A.; Diaz, A. V.; Moreno, M.; Santos, L.; Douhal, A. *J. Phys. Chem. A* **2001**, *105*, 7317. (b) Organero, J. A.; Moreno, M.; Santos, L.; Lluch, J. M.; Douhal, A. *J. Phys. Chem. A* **2000**, *104*, 8424. (c) Yamamoto, S.; Diercksen, G. H. F.; Karelson, M. *Chem. Phys. Lett*. **2000**, *318*, 590. (d) Nishimura, Y.; Tsuji, T.; Sekiya, H. *J. Phys. Chem. A* **2001**, *105*, 7273.

(27) (a) Mennucci, B.; Toniolo, A.; Tomasi, J. *J. Phys. Chem. A* **2001**, *105*, 4749. (b) Mennucci, B.; Toniolo, A.; Tomasi, J. *J. Phys. Chem. A* **2001**, *105*, 7126.

(28) Boys, S. F.; Bernardi, F. *Mol. Phys.* **1970**, *19*, 553.

(29) Frisch, M. J.; Trucks, G. W.; Schlegel, H. B.; Gill, P. M. W.; Johnson, B. G.; Robb, M. A.; Cheeseman, J. R.; Keith, T.; Petersson, G. A.; Montgomery, J. A.; Raghavachari, K.; Al-Laham, M. A.; Zakrzewski, V. G.; Ortiz, J. V.; Foresman, J. B.; Cioslowski, J.; Stefanov, B. B.; Nanayakkara, A.; Challacombe, M.; Peng, C. Y.; Ayala, P. Y.; Chen, W.; Wong, M. W.; Andres, J. L.; Replogle, E. S.; Gomperts, R.; Martin, R. L.; Fox, D. J.; Binkley, J. S.; Defrees, D. J.; Baker, J.; Stewart, J. P.; Head-Gordon, M.; Gonzalez, C.; Pople, J. A. *Gaussian 94*, revision E.2; Gaussian, Inc.: Pittsburgh, PA, 1995.

(30) Chou, P.-J.; Johnson, W. C., Jr. *J. Am. Chem. Soc*. **1993**, *115*, 1205.

(31) (a) Sobolewski, A. L.; Domcke, W. *Chem. Phys. Lett.* **1999**, *315*, 293. (b) Sobolewski, A. L.; Domcke, W. *Chem. Phys. Lett.* **1999**, *300*, 533. (c) Sobolewski, A. L.; Domcke, W. *Chem. Phys.* **2000**, *3259*, 181.

(32) Petke, J. D.; Maggiora, G. M.; Christoffersen, R. E. *J. Phys. Chem.* **1992**, *96*, 6992.

(33) Brealey, G. J.; Kasha, M. *J. Am. Chem. Soc.* **1955**, *77*, 4462.

(34) (a) Backer, R. S.; Kogan, G. *Photochem. Photobiol.* **1980**, *31*, 5. (b) Fujii, M.; Tamura, T.; Mikami, N.; Ito, M. *Chem. Phys. Lett.* **1986**, *126*, 583.

(35) (a) Lamola, A. A. *Photochem. Photobiol.* **1968**, 7, 619. (b) Lisewski, R.; Wierzchowski, W. L. *Chem Commun.* **1969**, 348. (c) Fisher, G. I.; Johns, H. E. *Photochem. Photobiol.* **1970**, *11*, 429.

(36) Kim, N. J.; Kang, H.; Jeong G.; Kim, Y. S.; Lee, K. T.; Kim, S. K. *J. Phys. Chem. A* **2000**, *104*, 6552.

(37) Krishna, V. G.; Goodman, L. *J. Am. Chem. Soc.* **1961**, *83*, 2042.

(38) Baba, H.; Goodman, L.; Valenti, P. C. *J. Am. Chem. Soc.* **1966**, *88*, 5410.

(39) Del Bene, J. E. *J. Mol. Struct.* **1984**, *108*, 179.